THE CATHARE CODE CONDENSATION MODELLING CONFRONTED TO THE TOPFLOW-PTS STEADY-STATE EXPERIMENTS

P.Gaillard, D.Bestion, I.Dor, P.Germain, F.Moutin
Commissariat à l'Energie Atomique
CEA-DEN-DM2S-STMF
17 rue des Martyrs, F-38054 Grenoble, France
gaillard.pierre@cea.fr, dominique.bestion@cea.fr, isabelle.dor@cea.fr, philippe-jm.germain@cea.fr, frederic.moutin@cea.fr

ABSTRACT

During a Loss Of Coolant Accident (LOCA) in a Pressurized Water Reactor (PWR), direct contact condensation (DCC) on a stratified flow may take place in the cold leg when the Emergency Core Cooling (ECC) system injects cold water. The condensation modeling of the system thermal-hydraulic code CATHARE-2 is compared to the experimental results from the new TOPFLOW-PTS tests, tests dedicated to condensation and mixing phenomena in cold leg. This is an opportunity to test and improve the scaling capabilities of the current model of the code.

The reference CATHARE condensation model was based on COSI data analysis and was then validated against various experimental data including LSTF and UPTF. This wide validation matrix covers a volume scaling factor from 1/100 to 1, includes both Large Break and Intermediate Break LOCA conditions and is now extended to TOPFLOW-PTS.

The present work revisits the physical mechanisms involved at the ECC injection and presents an improved condensation model with better scaling capabilities.

KEYWORDS
Condensation, CATHARE, Thermalhydraulic, Two phase flow, Heat exchange

1. INTRODUCTION

During a loss of coolant accident (LOCA), in a Pressurized Water Reactor (PWR), direct contact condensation occurs due to the Emergency Core Cooling (ECC) injection. Sub cooled water is injected into the cold legs in presence of a stratified flow. Following Bestion & Gros d'Aillon, 1989, Janicot 1992 and Janicot & Bestion 1993, three main condensation zones are identified:

i. Onto the ECC water jet itself , before impacting the free surface,
ii. On the free surface in the vicinity of the ECC impact with enhanced mixing due to jet induced turbulence
iii. On the free surface far from the jet influence.

Based on the previous works on the subject, this study proposes a new modeling of geometrical scale effects on the direct contact condensation in the vicinity of the ECC jet which provides better scaling

capabilities for the whole validation matrix. The CATHARE's reference validation matrix contains COSI, UPTF 8 and 25 and LSTF ROSA 1.1 tests.

The TOPFLOW-PTS tests, specifically dedicated to direct contact condensation and mixing study in the vicinity of the jet impinging, are added to this base. This large experimental condition range allows to see both integral and separate effect tests with a volume-power-flowrate scaling from 1/100 to 1 and injection flow rate values corresponding to small to large break LOCA.

The model developed in this study has been implemented in CATHARE 2, the French system code for nuclear thermal-hydraulic studies developed by CEA in a joint effort with AREVA, EDF and IRSN. It is based on the 6-equations 2-fluid model.

2. THE TOPFLOW-PTS TEST FACILITY

The Helmoltz-Zentrum Dresden-Rossendorf TOPFLOW-PTS (Peturaud, 2011) test facility is designed to investigate the mixing and Direct Contact Condensation (DCC) phenomena inside cold leg and downcomer during injection of sub-cooled ECC in the frame of Pressurized Thermal Shock investigations. The French CPY 900 MWe reactor was used as reference plant. The geometrical scale of the test facility is 1:2.5.

The experimental facility is composed by:

i. a pump simulator,
ii. a cold leg,
iii. an ECC nozzle
iv. a flat downcomer portion which represents 90° of the reactor downcomer,
v. a water level regulation,
vi. a pressure regulating boiler.

The test section is installed in a pressure vessel, the so-called "diving tank" (Péturaud, 2011) to be in pressure equilibrium with its environment. The tests can be operated up to 5 MPa, the pressure in the test rig being controlled by steam injection. The water level is regulated at constant values (0, 25, 50, 75 and 100% of cold leg diameter).

The condensation model development used the steady state steam-water (sssw) tests which cover different operational condition for pressure, injection flow rate, and sub cooling.

The instrumentation includes thermocouples, infra-red camera, flow meter, pressure sensor and wire mesh sensor. With the aim of analyzing the mixing phenomenon and the cold leg condensation, thermocouples lances are arranged in the cold leg at different sections. Thanks to these measurement points, the thermal behavior in the cold leg can be studied.

The condensation flow rate for each test is determined by an energy balance applied to the steam regulation system. Several measured parameters are used for the condensation flow rate calculation: inlet and outlet steam flow rates, pressure and temperature in the circuit.

These tests are used in order to define the new condensation model developed in this paper. The next paragraphs detail the model development and then the validation realized against specific tests.

3. THE DATA BASE USED IN THIS MODEL DEVELOPMENT

The condensation model developed in this paper used the TOPFLOW-PTS data and all other data of the CATHARE validation matrix listed here below (see Table I).

The COSI experiment (separate effect test) is the experiment which was used to develop the CATHARE reference condensation model. It was especially dedicated to condensation at ECC injection in the cold leg. It was scaled at 1/100 for volume and power from a 900 MWe water reactor. The facility consisted of a scaled cold leg and a downcomer, simulated by a vertical pipe. Two test sections, one for the FRAMATOME cold leg design and another for the WESTINGHOUSE cold leg design were used. Different injection pipes were used.

LSTF (Large Scale Test Facility) is an integral effect facility, operated by JAERI in Japan. It is a 4 loops reactor scaled at 1/48 for volume and 1 for height. The ROSA 1.1 tests consist of different injection stages in the cold leg in order to study the condensation and the thermal stratification in the cold leg. During the different stages of the ROSA 1.1 experiment, cold leg level and injection flow rate are adjusted. Thermocouple lances are put at the cold leg outlet in order to track the liquid temperature, influenced by condensation and mixing between ECC and cold leg main flow.

UPTF (Upper Plenum Test Facility) facility (integral effect test) is a full scale 4-loops reactor designed by SIEMENS and operated by KWU. It is based on a 1300 MWe design. The tests 8 and 25 study the refill and reflooding processes. Each test is split in 2 runs, A and B which have very close experimental conditions. In each run, there are 6 ECC injection flowrate stages where the injection flow rate in the cold leg is modified in order to analyze the temperature behavior at the downcomer inlet. As for LSTF ROSA 1.1, the test facility supports thermocouple lances at the cold leg outlet for liquid temperature measurement.

Table I. Experimental conditions for the condensation model design

	ECC flow rate	ECC temperature	Pressure	Saturation temperature	ECC sub-cooling	Cold leg level	ECC diameter (d_{ECC})	Cold leg diameter (Dh)
	[kg/s]	[°C]	[Mpa]	[°C]	[°C]	[%]	[m]	[m]
COSI	[0,1 ; 0,6]	[18,5 ; 84]	[2,1 ; 7,1]	[212,3 ; 285,8]	[187,3 ; 263,8]	[0 ; 0,6]	[0,006 ; 0,038]	0,118
TOPFLOW	[0,7 ; 2,5]	[113,7 ; 243,9]	[3 ; 5]	[233,8 ; 264]	[5 ; 120,2]	[0 ; 0,8]	0,053	0,279
UPTF	[80 ; 600]	[29 ; 38]	[0,3 ; 0,4]	[127,4 ; 142,7]	[97,4 ; 108,7]	[0,1 ; 0,5]	0,349	0,75
LSTF	[0 ; 1]	[37 ; 266]	[15,4 ; 15,4]	[344,1 ; 344,1]	[78 ; 307,1]	[0,5 ; 0,8]	0,025	0,207

	d_{ECC} / D_h	Reynolds number	Froude number	Prandtl number
COSI	[0,05 ; 0,32]	[13942 ; 443395]	[0,4 ; 13,7]	[0,7 ; 0,8]
TOPFLOW	0,19	[139845 ; 502807]	[0,3 ; 1]	[0,7 ; 0,8]
UPTF	0,465	[1208 ; 10560000]	[0,001 ; 3,2]	[1,2 ; 1,3]
LSTF	0,121	[6839 ; 42522]	[0,4 ; 3,2]	[0,6 ; 0,7]

4. DIRECT CONTACT CONDENSATION PHENOMENA

The initial COSI data analysis and condensation modeling was presented by Janicot & Bestion 1993. The flow in the cold leg is stratified. The ECC injects and three main condensation zones are identified (see Figure 1). This zone segmentation has been introduced by Bestion and Gros d'Aillon 1989. The ECC injection impacts the stratified free surface. This creates strong perturbations on the water-steam free surface and increases the local condensation. Some important DCC phenomena were pointed-out:

i. The amount of vapor condensed depends strongly on: the injected mass flow rate, the water level in the cold leg and the ECC sub-cooling,
ii. Some sub-cooled liquid is present upstream of the injection point. It testifies to a recirculation cell upstream of the injection,
iii. An important part of the condensation occurs in the very vicinity of the injection.

The DCC modeling includes three terms:

i. Condensation on the jet itself due to sub cooled water injected in a vapor flow (Zone B),
ii. Condensation at the free surface enhanced by the turbulence created by the ECC jet when it impacts the free surface of the main flow (Zone B),
iii. Condensation at the free surface in Zone C.

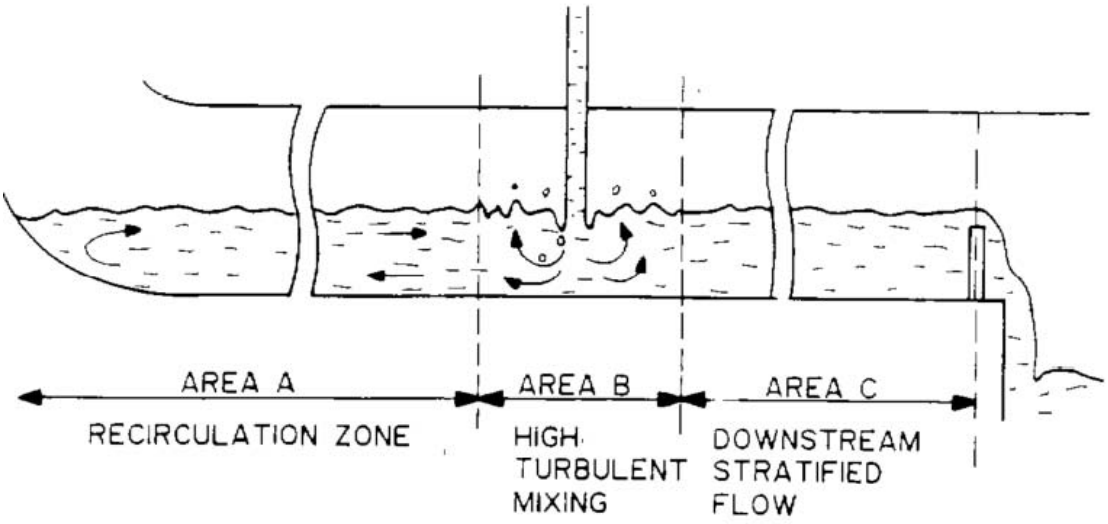

Figure 1. Condensation zones in the cold leg – From [1]

In the zone A upstream of injection, since there is no net flowrate in steady state, a 1D model cannot predict the condensation as it cannot represent the recirculation.

The main part of the condensation flow rate is generated in the vicinity of the jet impact (Zone B). Indeed, the liquid flow temperature measured one hydraulic diameter downstream the injection is very close to the temperature measured at the downcomer inlet. The model developed here after concerns especially this region B and models the heat flux due to the turbulence created by the jet impact: the main condensation term. The condensation modeling in this zone B is detailed in the next paragraph.

5. DCC MODEL IN THE VICINITY OF INJECTION

The reference model is the standard CATHARE-2 code Janicot and Bestion 1993 model (this reference model terms are detailed in the Table II). The TOPFLOW-PTS tests give the opportunity to improve the model scaling. Previous CATHARE 2 validation on LSTF ROSA 1.1 and UPTF 8 & 25 had shown that the scale effect in the reference model could be improved. The matrix extension with different experimental scales will help understanding what geometrical scales control the DCC phenomena.

The heat flux at the interface is function of the heat transfer coefficient h (W/m^2/K), the interfacial area A_i (m^2) and the main flow sub-cooling $\Delta T = T_{sat} - T_L$ (K)

$$\varphi = A_i . h . \Delta T \quad (1)$$

The phenomena which are induced by the jet are the following:

i. The plunging jet creates an entrainment of free surface water with converging streamlines towards the jet (see Figure 2). This free surface velocity plays a role in the enhanced condensation efficiency in the vicinity of the jet.
ii. The jet splitting at the bottom wall creates a rebound along the side walls with waves which also create significant perturbations at the free surface (Figure 2),
iii. The jet below the free surface creates some upstream and downstream flow at the bottom but also some kind of circulation cells as shown in Figure 3 (left). This induces also a velocity at the free surface over an axial distance equal to the jet diameter (Figure 3, right).

Looking for a model for the region B, the first question is to define what the free surface area affected by the enhanced heat transfer is. If the cold leg diameter (D_h) is considered large enough compared to the injection diameter (d_{ECC}), the heat exchange area influenced by the jet should be independent on D_h and only be proportional to d_{ECC}^2.

$$A_i \sim d_{ECC}^2 \quad (2)$$

If the circulation cell mentioned above is the dominant effect, the affected free surface area might be proportional to $D_h d_{ECC}$.

The heat exchange coefficient can be expressed in function of the Nusselt number:

$$h = \frac{\lambda_L Nu}{l_t} \quad (3)$$

With :
λ_L : the liquid thermal conductivity (W/m.K)
Nu : the Nusselt number
l_t : the turbulent length scale of the phenomena (m).

The subscript L refers to the liquid in the injection mesh which results from the mixing between the cold leg flow and the injection flow.

As in Bankoff works (Kim, Lee and Bankoff 1985) , the Nusselt number can be expressed as function of the turbulent Reynolds number (Re_t) and the Prandtl number (Pr) of the flow:

$$Nu = \frac{h l_t}{\lambda_L} = K . Re_t^a . Pr^b \quad (4)$$

With: $Re_t = \frac{\rho_L . V_t . l_t}{\mu_L}$ and $Pr = \frac{\mu_L Cp_L}{\lambda_L}$
ρ_L : liquid density (kg/m^3)
V_t : turbulent velocity scale (m/s)
l_t : turbulent length scale (m)
μ_L : liquid viscosity (Pa.s)
Cp_L : liquid thermal capacity (J/kg.K)
K: a constant
a : a constant
b : a constant

The turbulent length scale (l_t) is used in order to define both the Nusselt and the Reynolds numbers. It is proportional to d_{ECC} if the free surface entrainment is dominant or proportional to the liquid height if the recirculation cell is dominant. Following Janicot & Bestion 1993, it is assumed here that the turbulent length scale is governed by the liquid height in the cold leg. The liquid height in the cold leg is approximated as a liquid fraction linear function:

$$l_t = D_h(1 - \alpha) \quad (5)$$

With :
D_h : the cold leg hydraulic diameter (m)
α : the void fraction

In case of a SBLOCA, the injection velocity is much higher than cold leg flow velocity. The ECC velocity prevails on the local turbulence close to the injection. That is why the injection velocity is considered as the turbulent velocity scale. This seems valid if the free surface entrainment is dominant or even if the recirculation cell effect is dominant.

$$V_t \equiv V_{ECC} \quad (6)$$

However some phenomena such as the jet bouncing and wave formation along the side walls are not modelled in the Nusselt formulation shown in (4). As depicted in Figure 2and Figure 3, the mixing consists of several phenomena:

i. Turbulence development in the water height (vertically) in the jet impinging vicinity,
ii. A liquid layer flows from the bottom of the pipe and rises up along the cold leg wall. This flow, created by the injection, increases the heat exchange area because it flows above the free surface (Figure 2 right). The height achieved by this flow along the wall is called rebound height (h_R).
iii. The jet kinetic energy dissipation before bringing back turbulence close to the free surface affects the efficiency of the condensation.

The turbulence development is translated by the general Nusselt number formulation (4), especially by the Reynolds number.

The jet bouncing effect is added by an effect of a Froude Number defined by (7) :

$$Fr = \frac{V_{ECC}}{\sqrt{gl}} \quad (7)$$

With:
g: the gravity acceleration (m/s²)

The length scale l is defined by (5), the ratio $\sqrt{\frac{V_{ECC}^2}{g}}$ corresponds to the rebound height of the jet. This Froude number is then the ratio between the rebound height and the water height in the cold leg:

$$Fr = \sqrt{\frac{h_R}{D_h(1-\alpha)}} \qquad (8)$$

An effect of Fr translates the fact that the higher the rebound compared to the water height, the more the exchange area is disrupted. The jet impinging waves influence the exchange area or improve the transfer coefficient. They increase the heat exchange.

The jet kinetic energy dissipation before bringing back turbulence close to the free surface is probably a complex function of the cold leg, the ECC geometries and the water height. The jet turbulence will be more effective if the ECC diameter is close to the cold leg diameter and if the water height is not too high avoiding too much dissipation. One expects an efficiency increasing with α, and with $\frac{d_{ECC}}{D_h}$. This effect is taken in account in the Nusselt number coefficient by $f(\alpha, \frac{d_{ECC}}{D_h})$. The new general Nusselt formulation is then supposed to be:

$$Nu = K.Re_t^a.Pr^b.Fr^c.\alpha^d.(\frac{d_{ECC}}{D_h})^e \qquad (9)$$

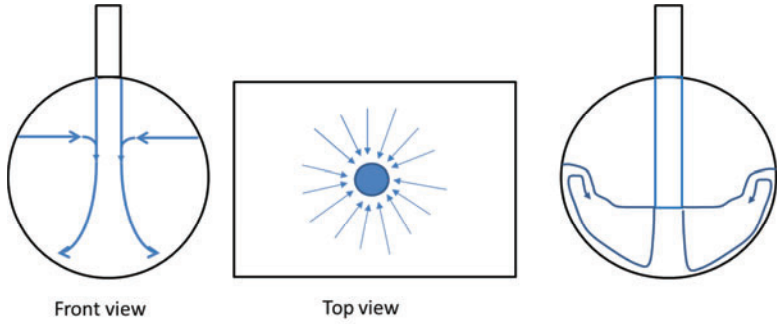

Figure 2. Jet impact on free surface flow; entrainment of free surface water by the plunging jet (left and middle) and creation of a wave on side walls (right) by jet bouncing on bottom wall

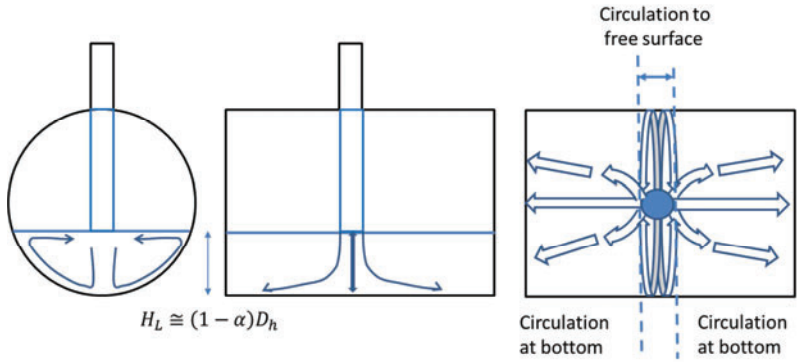

Figure 3. Velocity induced by the jet along the cold leg walls : front view (left), side view (middle) and top view (right)

The exponents a, b, c , d, e and the constant K in the equation (9) are defined in order to fit the experimental data from the different facilities taken in account for this model definition: COSI experiments (both WESTINGHOUSE and FRAMATOME test section), TOPFLOW-PTS steady state tests and UPTF 8 & 25. The general experimental conditions for these tests are introduced in Table I.

The Figure 4 shows the following expression: $\frac{Q_{cond}L_v\mu_L}{\lambda_L\rho_L\Delta T} \sim A_i.Nu$ based on measured data.

The evaluation of the experimental value is made with a rather high uncertainty since measured temperature values do not give the energy flowrate in absence of velocity measurements. But it was supposed that the qualitative trends could be identified.

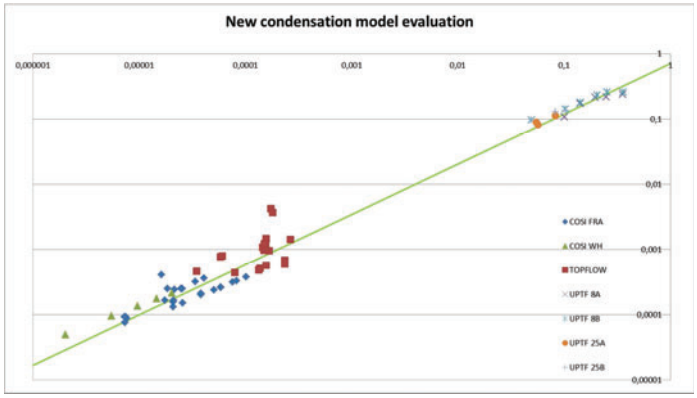

Figure 4. Experimental versus calculated Ai.Nu

The assumption of $A_i \sim d_{ECC}^2$ was first used.

Surprisingly after several attempts, d=e=1 were simple values which provided good agreement. It is consistent with two possible interpretations:

i. $A_i \sim d_{ECC}^2 \; and \; e = 1$
ii. $A_i \sim d_{ECC} D_h \; and \; e = 2$

Then, the model is implemented in CATHARE 2 V2.5_3 mod 3.1. The COSI, TOPFLOW-PTS, UPTF 8 & 25 and ROSA LSTF 1.1 tests have been calculated. The Table II summarizes the principal terms for both condensation model, the reference model and the new one.

Table II. Condensation model terms comparison

	Reference model	New condensation model
Heat exchange area	$D_h^2.\alpha$	$d_{IS}^2.\alpha$
Turbulent Reynolds number	$Re_t = \frac{\rho_L V_{IS} d_{IS}}{\mu_L}$	$Re_t = \frac{\rho_L V_{IS} L_t}{\mu_L}$
Nusselt number	$Nu = A1.Re_t$	$Nu = A3.\frac{d_{IS}}{D_h}.Re_t.Pr^b.Fr^c$
Heat transfer coefficient	$h = \frac{\lambda_L Nu}{D_h}$	$h = \frac{\lambda_L Nu}{L_t}$
Turbulent length scale	-	$L_t = D_h(1-\alpha)$

For the COSI and TOPFLOW-PTS, separate effect tests, the measured condensation flow rate is compared to the calculated condensation with CATHARE. The calculations with the reference CATHARE model for COSI were already rather good. The mean relative difference between experimental data and calculations was 9.4%. With the new length scale, it is reduced to 8.4%. For TOPFLOW-PTS steam-water steady-state tests, this mean relative difference between experimental measures and calculation with the reference model was 47.4%. This new approach reduces the difference to 25% which is the value of the measurement uncertainty (+/-25%).

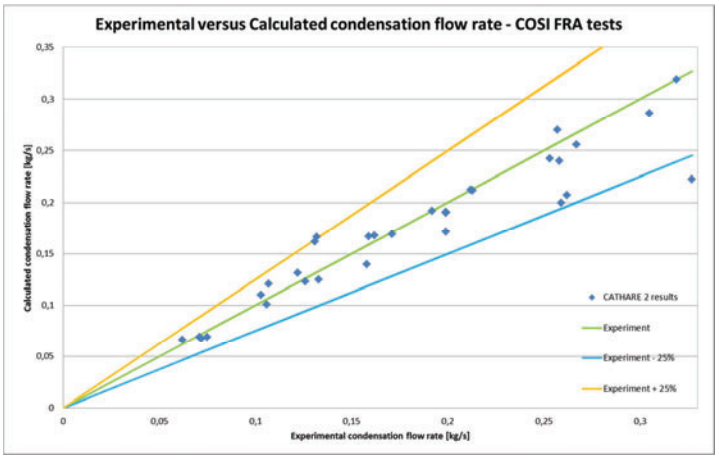

Figure 5. Experimental versus calculated condensation flow rate for COSI tests

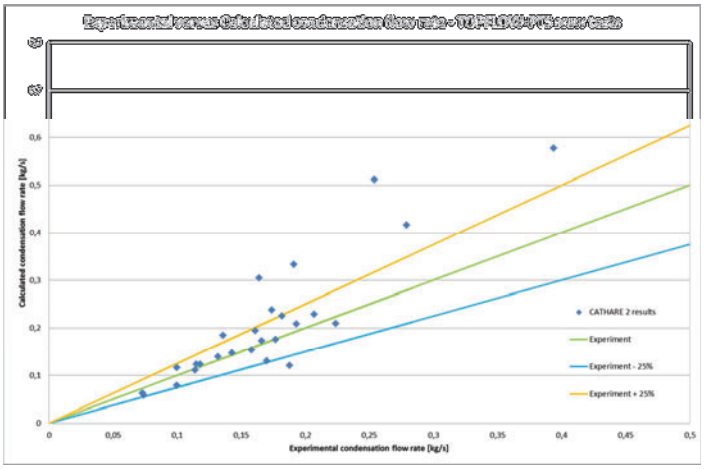

Figure 6. Experimental versus calculated condensation flow rate for TOPFLOW-PTS sssw tests

About LSTF ROSA 1.1 tests, the CATHARE results with the reference model were already rather accurate. The new model doesn't degrade the predictions. The results are summarized in Figure 7 and Figure 8. The temperature evolutions for all tests are not summarized in this paper.

i. LSTF Test AB5 : This test is not disrupted by the new condensation model. The results are already very accurate with the reference model. The results with the new model are nearly the same.

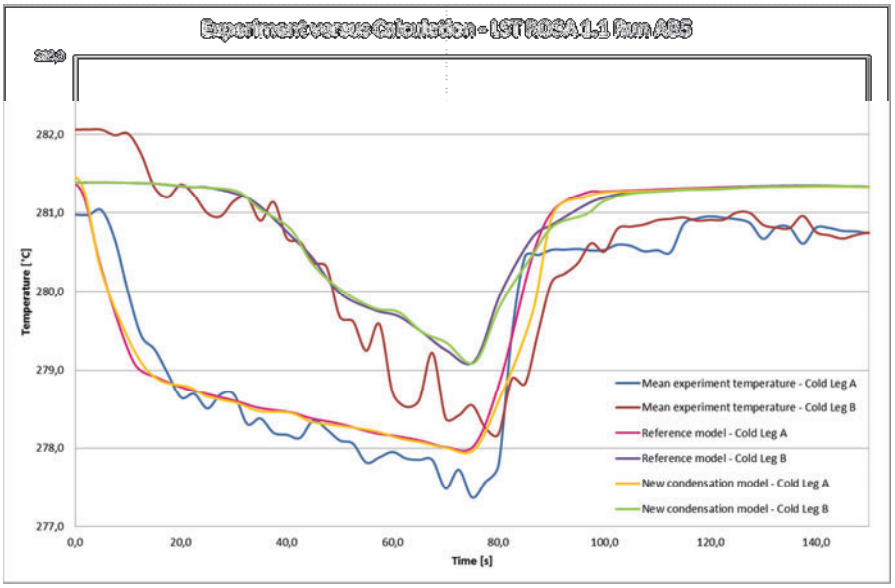

Figure 7. Experimental versus calculated temperature in DC entry for LSTF ROSA 1.1 AB5 test

ii. LSTF Test AB6 : As for test AB5, the results, already satisfactory are very slightly modified. Where the reference model is efficient, the new model is efficient also.

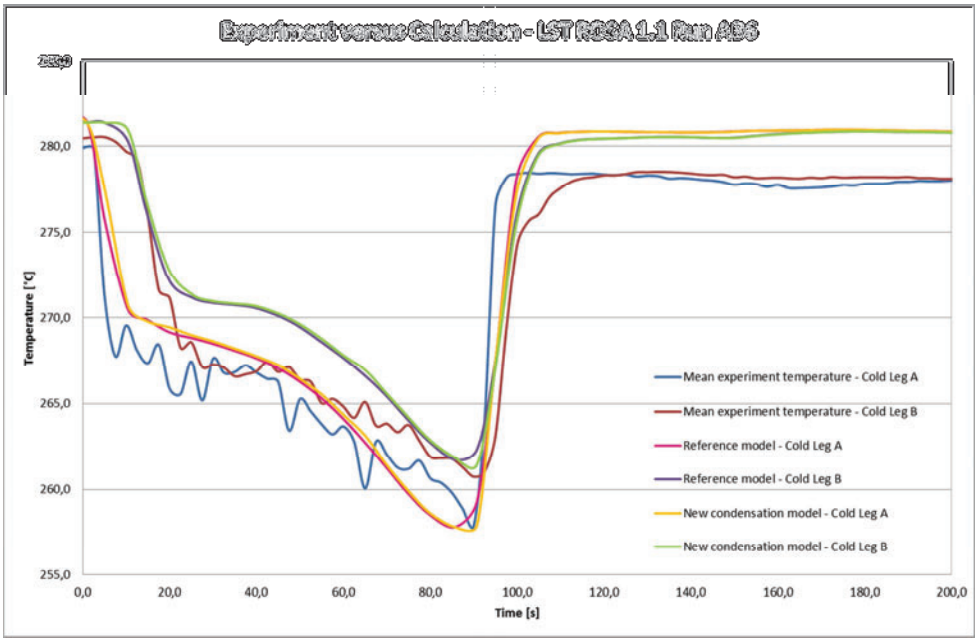

Figure 8. Experimental versus calculated temperature in DC entry for LSTF ROSA 1.1 AB6 test

The LSTF tests AB5 and AB6 conditions are detailed in the Table III.

Table III. Experimental conditions for the LSTF AB5 and AB6 tests

	LSTF AB5 Test	LSTF AB6 Test
Primary pressure [bar]	67,4	67,4
Steam-generator pressure [bar]	63	63
Primary flow rate [kg/s]	10,9	10,7
Steam generator level [m]	9,7	9,7
Cold leg level [%]	80	80
ECC flow rate [kg/s]	5	6

The CATHARE calculations for UPTF 8A, 8B, 25A and 25B could be improved. Here after is an analysis for each UPTF run studied for this model development. The experimental conditions for UPTF tests are summarized in Table IV.

Table IV. Experimental conditions for the UPTF 8A/B and 25A/B tests

	8A					
Primary pressure [bar]	3,9					
Saturation temperature [°C]	142,7					
Initial level in the test vessel [m]	4					
ECC flow rate [kg/s]	600	410	250	200	150	80
ECC temperature [°C]	30					

	8B					
Primary pressure [bar]	3,9					
Saturation temperature [°C]	142,7					
Initial level in the test vessel [m]	4					
ECC flow rate [kg/s]	600	410	250	200	150	80
ECC temperature [°C]	30					

	25A			25B		
Primary pressure [bar]	2,5			2,5		
Saturation temperature [°C]	127,4			127,4		
Initial level in the test vessel [m]	4			4		
ECC flow rate [kg/s]	115x3	80x3	80x3	115x3	80x3	142x3
ECC temperature [°C]	30			30		

i. UPTF 8A (Figure 13): The difference between calculation and measures is up to 30°C with the reference model on the fourth injection stage. This value is the maximum difference during 8A test. The mean difference is around 20°C. With the new approach, the calculation results are much more accurate. The maximal gap between calculated and measured temperature is 9°C, the mean difference with the new condensation model is slightly higher than 7°C.

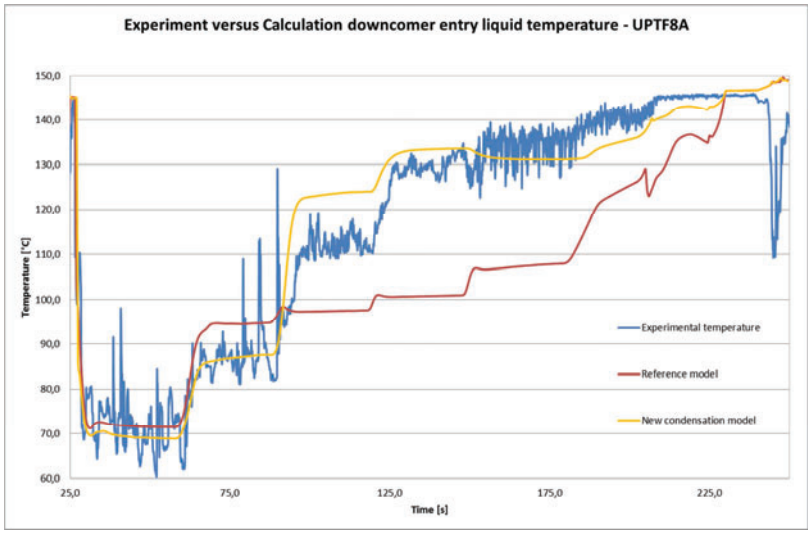

Figure 13. Experimental versus calculated temperature in downcomer entry for UPTF 8A test

ii. UPTF 8B (Figure 14): This run has more or less the same behavior than UPTF 8A. The reference model results verify a maximum temperature difference of 20°C. The new model allows to reduce this temperature difference to 8°C.

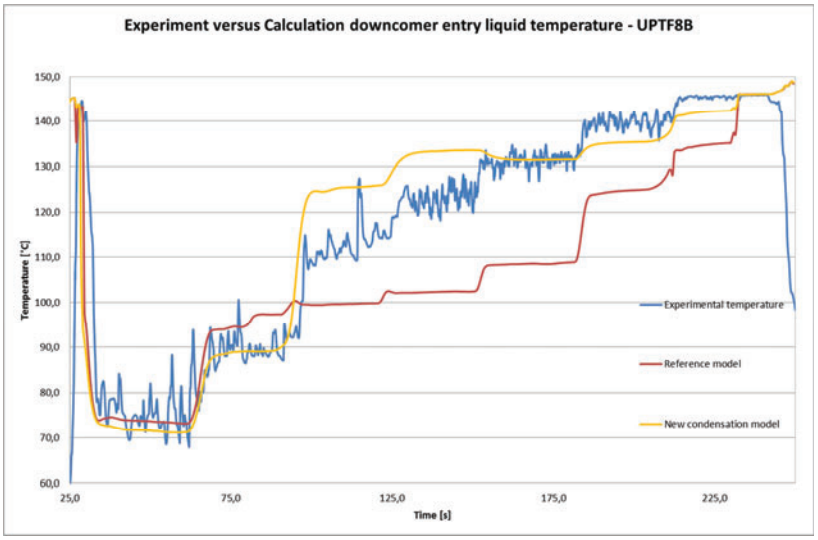

Figure 14. Experimental versus calculated temperature in downcomer entry for UPTF 8B test

iii. UPTF 25A (Figure 15): From the first stage of this run, the difference between the reference calculation and the measures is about 30°C. On the following stages, the temperature difference is around 20°C. With the model developed in this study, the prediction performances are improved a lot. The maximum temperature difference reaches 8°C and the mean difference is 5°C.

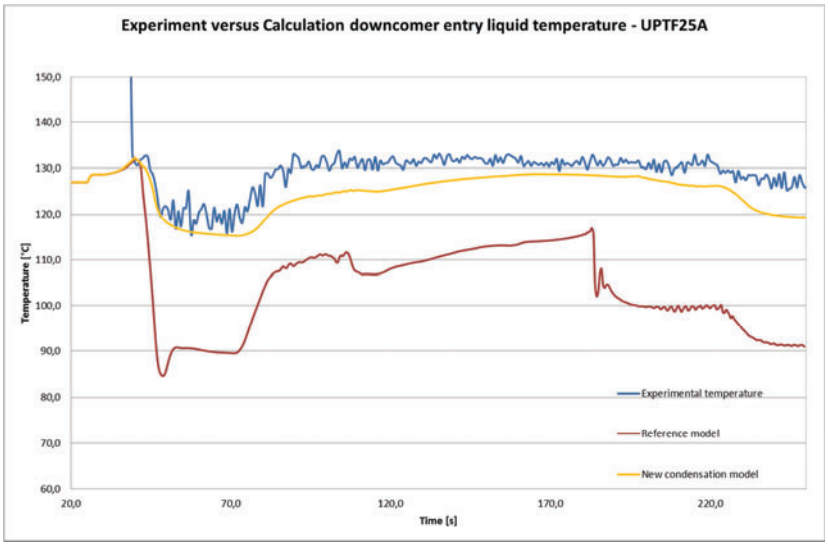

Figure 15. Experimental versus calculated temperature in downcomer entry for UPTF 25A test

iv. UPTF25B (Figure 16): The experimental conditions are very close to UPTF 25A, that's why the results are nearly the same. With the reference model, the temperature difference for the first stage is higher than 20°C and stays around this value during the rest of the test. With the new model, the maximum temperature difference doesn't exceed 7°C. The mean difference is 5°C.

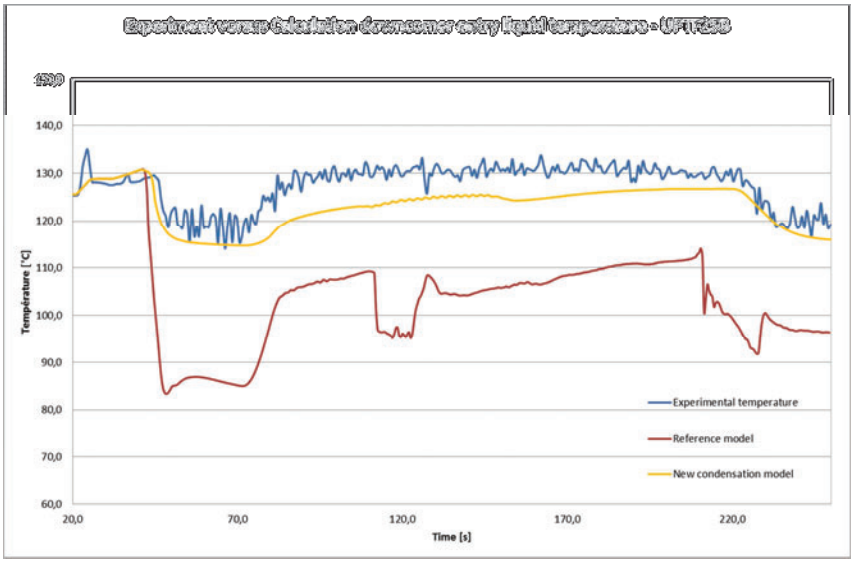

Figure 16. Experimental versus calculated temperature in downcomer entry for UPTF 25B test

6. CONCLUSIONS

The TOPFLOW-PTS data are used to improve the condensation model at ECC injection of the CATHARE-2 code. In order to better identify the geometrical scale effects on the local condensation in the vicinity of the ECC, data at different scales were considered including COSI, TOPFLOW, LSTF and UPTF data.

A new model is proposed which is as good as or better than the current model in COSI and LSTF and which is much better for TOPFLOW and UPTF.

The new model is based on a unified length scale for both turbulent flow modeling and turbulent heat transfer. This point is main progress regarding to the reference model where the turbulence model is not the same according to the phenomenon modeled.

This model development, based on a wide data base with a large scale range allows to end on a robust model which has been confronted with succeed against tests from scale 1/100 to 1 and with ECC injection flow rate representative of small to large break LOCA. This new scale approach improves the results where it is needed and stays as accurate as the reference model where this one is already efficient.

REFERENCES

1. Bestion & Gros d'Aillon 1989 – Condensation tests and interpretation – The CATHARE condensation model – NURETH 4, Karlsruhe
2. Janicot 1992 – Condensation modelling for ECC injection – CNSI Specialist Meeting on "Transient Z-phase flow", Aix en Provence
3. Janicot, D. Bestion, Condensation modelling for ECC injection, Nuclear. Engineering. & Design, 145 (1993) 37-45
4. Péturaud & al. 2011 – General overview of the TOPFLOW-PTS experimental program – NURETH 14, Toronto
5. Kim, Lee and Bankoff 1985 – Heat transfert and interfacial drag in countercurrent steam water stratified flow – Journal of multiphase flow Vol 11, N°5, pp 593-606

NOMENCLATURE

A_i : Interfacial heat transfer area [m²]
Cp_L : Liquid heat capacity [J.kg^{-1}.K^{-1}]
D_h : Hydraulic diameter [m]
Fr : Froude number
K : Constant
Pr : Prandtl number

a : Constant
b : Constant
d_{ECC} : Emergency core cooling injection diameter [m]
g : Gravity acceleration [m.s^{-2}]
h : Heat transfer [W.K^{-1}]
h_R : Rebound height [m]
l_t : Turbulent length scale [m]
l_v : Specific heat [J.kg^{-1}]

Q_{cond} : Condensation flow rate [kg.s^{-1}]

Re : Reynolds number
V_t : Turbulent velocity scale [m.s^{-1}]
V_{ECC} : Emergency core cooling velocity [m.s^{-1}]

DCC : Direct Contact Condensation
ECC : Emergency Core Cooling
LOCA : Loss Of Coolant Accident
LSTF : Large Scale Test Facility
MWe : Electrical Megawatt
PWR : Pressurized Water Reactor
UPTF : Upper Plenum Test Facility

ΔT : Temperature difference [°K]

α : Void fraction
λ_L : Liquid conductivity [W.m^{-1}.K^{-1}]
ρ_L : Liquid density [kg.m^{-3}]
μ_L : Liquid viscosity [Pa.s]